Novel fluorescent triazinobenzimidazole derivatives as probes for labelling human A_1 and A_{2B} adenosine receptor subtypes.

Elisabetta Barresi[a,†], Chiara Giacomelli[a,†], Simona Daniele[a], Ilaria Tonazzini[b], Marco Robello[c], Silvia Salerno[a], Ilaria Piano[a], Barbara Cosimelli[d], Giovanni Greco[d], Federico Da Settimo[a], Claudia Martini[a], Maria Letizia Trincavelli[a,*], Sabrina Taliani[a]

[†] These Authors contributed equally.

[a]*Dipartimento di Farmacia, Università di Pisa, Via Bonanno 6, I-56126 Pisa, Italy*
[b]*Istituto Nanoscienze-CNR @NEST (National Enterprise for NanoScience and NanoTechnology), Piazza San Silvestro 12, Pisa, Italy*
[c]*NIDDK (National Institute of Diabetes and Digestive and Kidney Diseases), NIH, 8 Center Drive, Bethesda, MD 20814*
[d]*Dipartimento di Farmacia, Università di Napoli "Federico II", Via Domenico Montesano 49, 80131 Naples, Italy.*

** Email: maria.trincavelli@unipi.it; Tel: +39 050 2219523*

Keywords: Adenosine receptors; fluorescent probes; triazinobenzimidazole derivatives; mesenchymal stem cells; A_{2B} AR subtype.

Abstract

The expression levels and the subcellular localization of adenosine receptors (ARs) are affected in several pathological conditions as a consequence of changes in adenosine release and metabolism. In this respect, labelled probes able to monitor the AR expression could be a useful tool to investigate different pathological conditions. Herein, novel ligands for ARs, bearing the fluorescent 7-nitrobenzofurazan (NBD) group linked to the N^1 (**1**,**2**) or N^{10} (**3**,**4**) nitrogen of a triazinobenzimidazole scaffold, were synthesized. The compounds were biologically evaluated as fluorescent probes for labelling A_1 and A_{2B} AR subtypes in bone marrow-derived mesenchymal stem cells (BM-MSCs) that express both receptor subtypes. The binding affinity of the synthetized compounds towards the different AR subtypes was determined. The probe **3** revealed a higher affinity to A_1 and A_{2B} ARs, showing interesting spectroscopic properties, and it was selected as the most suitable candidate to label both AR subtypes in undifferentiated MSCs.

Florescence confocal microscopy showed that compound **3** significantly labelled ARs on cell membranes and the fluorescence signal was decreased by the cell pre-incubation with the A_1 AR and A_{2B} AR selective agonists, R-PIA and BAY 60-6583, respectively, thus confirming the specificity of the obtained signal. In conclusion, compound **3** could represent a useful tool to investigate the expression pattern of both A_1 and A_{2B} ARs in different pathological and physiological processes. Furthermore, these results provide an important basis for the design of new and more selective derivatives able to monitor the expression and localization of each different ARs in several tissues and living cells.

1. Introduction

In last decades, the use of fluorescent probes for studying membrane G-coupled protein receptors (GPCRs) has gained great importance. Given the recent improvements in imaging technologies, fluorescent probes have become attractive alternatives to radioligands, which are inevitably associated with peculiar drawbacks, such as high costs and risks related to handling radioactive materials.[1,2]

Ideally, a fluorescent probe should retain the pharmacological profile of the parent unlabelled ligand so as to guarantee optimal conditions for binding studies, including cellular localization and real-time monitoring of processes triggered by ligand-receptor interactions in living cells (i.e. internalization, trafficking, sequestration and recycling, identification of ligand binding site).[1,2]

Various fluorescent probes have been developed over the past few years for characterizing adenosine receptors (ARs), and their use in fluorescence resonance energy transfer (FRET), confocal analysis and flow cytometry (FCM) has been proven feasible.[3-5]

The nucleoside adenosine plays an important role in many physiological and pathological conditions through activation of specific GPCRs, classified as A_1, A_{2A}, A_{2B}, and A_3 ARs.[6,7] The binding of adenosine to ARs activate G protein-dependent signalling pathways, such as adenylate cyclase (A_1, A_{2A}, A_{2B} and A_3 ARs), calcium or potassium channels (A_1 AR), phospholipase C (A_1, A_{2B} and A_3 ARs) and phospholipase D (A_3 AR),[6,7] cascade of mitogen-activated protein (MAP) kinases (A_1, A_{2A} and A_{2B} ARs).[8-10]

Over the past decades, we have been working on several classes of ligands binding with high affinity and selectively to various AR subtypes, most of them characterized by an antagonist efficacy profile.[11-21]These classes share common structural features consisting in an aromatic polycyclic nitrogen-containing core bearing mostly lipophilic substituents and, less often, groups capable to make hydrogen bonds. In some cases, different substitution pattern on the same scaffold yielded compounds with switched selectivity from one receptor subtype to a different one.[11-13,17,18] Among the ARs-targeting scaffolds, the triazinobenzimidazole system (general structure **I**, Chart 1), originally used for the identification of ligands for the central benzodiazepine receptor,[22] was then employed to obtain potent and selective A_1 AR antagonists.[11,12] Subsequently, potent triazinobenzimidazole-based A_{2B} AR antagonists were disclosed with scarce or moderate affinity for A_3 and A_1 ARs, their degree of A_{2B}/A_{2A} AR selectivity being

strictly dependent on the nature of the aryl group at the 3-position of the scaffold.[18] More recently, based on this chemotype, a novel carbon-11 labelled tracer was synthesized and tested by positron emission tomography (PET) to evaluate its pharmacokinetics in vivo, and to ascertain its potential use for A_{2B} AR imaging.[23] As a result, we identified a probe with a high chemical stability, a good pharmacokinetic profile, and the ability to image A_{2B} AR. Such a compound represents the first A_{2B} AR targeting PET tracer disclosed so far.[23] Taken together, all these findings supported the potential usefulness of the triazinobenzimidazole scaffold **I** (Chart 1) in the design of novel ARs ligands suitable as molecular probes for imaging experiments.

Recent evidences indicate that adenosine plays a crucial role in mesenchymal stem cell (MSC) biology by controlling the fates of these cells.[24] MSCs are multipotent stem cells that can differentiate into osteoblasts and adipocytes.[24] It has been reported that MSCs express various AR subtypes,[24,25] whose expression differently varies during the differentiation process.[24]

Specifically, in human bone marrow-derived (BM)-MSCs, A_{2B} AR is the dominant receptor promoting osteoblast differentiation, as demonstrated by an increase in alkaline phosphatase activity Runx2 expression.[24-26] D'Alimonte et al.[27] have demonstrated that activation of A_1 AR promotes osteogenic differentiation of human dental pulp-derived MSCs, similarly to what observed upon A_{2B} AR activation. According to Eisenstein, A. et al.,[28] A_1 and A_{2A} ARs are implicated in the regulation of BM-MSC differentiation to adipocytes.

Although the role of ARs in lineage-specific differentiation of MSCs is widely accepted, the specific involvement of A_1 and A_{2B} ARs in the different phases of differentiation and the related underlying mechanisms are still unclear.

The present paper describes our studies aimed at developing novel triazinobenzimidazole fluorescent ligands of human ARs as suitable tools to monitor the evolution of AR expression during early stage of BM-MSC differentiation to osteoblasts. Specifically, herein we report the synthesis, the spectroscopic properties and the biological evaluation of novel probes **1**-**4**, bearing the fluorescent moiety linked to the N^1 (compounds **1**,**2**) or N^{10} (compounds **3**,**4**) nitrogen (Chart 1) of the triazinobenzimidazole scaffold. The position and the length of the spacer chain were modified to modulate conformational flexibility required to self-adaptation of the molecules into the receptor binding site. The well-known 7-nitrobenzofurazan (NBD) group was selected as the fluorophore for its small sizes. Moreover, thanks to the

solvatochromic properties of NBD, NBD-containing compounds typically exhibit a low quantum yield in aqueous solutions, but they become highly fluorescent in nonpolar solvents or when bound to membranes as well as to protein hydrophobic clefts.[29] This fluorophore was successfully employed by our group for developing highly performant fluorescent probes specifically targeting the translocator protein (TSPO).[30-32] Indeed, a NBD-containing TSPO ligand has been successfully used to detect the TSPO mitochondrial localization in cultured Drosophila S2 cells.[33]

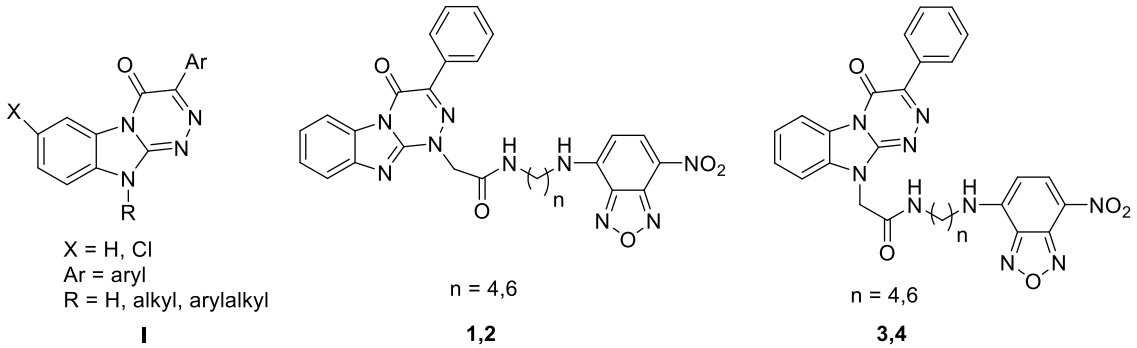

Chart 1. Structures of triazinobenzimidazole ARs ligands **I**[11,12,18] and fluorescent probes **1**-**4**.

2. Results and Discussion

2.1. Chemistry

The target compounds **1**,**2** and **3**,**4** were synthesized using the triazinobenzimidazoles **9** and **10** as reactants, respectively, which in turn were prepared starting from compound **8**; this last product was obtained according to the experimental procedure described in our previous work (Scheme 1).[22] Briefly, 2-hydrazinobenzimidazole (**6**) was synthesized from hydrazine monohydrate and 2-chlorobenzimidazole (**5**) and then reacted with phenylglyoxylic acid in absolute ethanol to give the intermediate **7**, which was finally cyclized by refluxing for 12 hours in glacial acetic acid, yielding compound **8**.[22]

Due to the tautomeric equilibrium involving **8**, treatment of this compound with sodium hydride and ethyl bromoacetate induced the alkylation at the N^1 or N^{10}, affording a mixture of the regioisomer derivatives **9** (yield 51%) and **10** (yield 22%), respectively, which were finally separated and purified by flash chromatography (Scheme 1).

Scheme 1

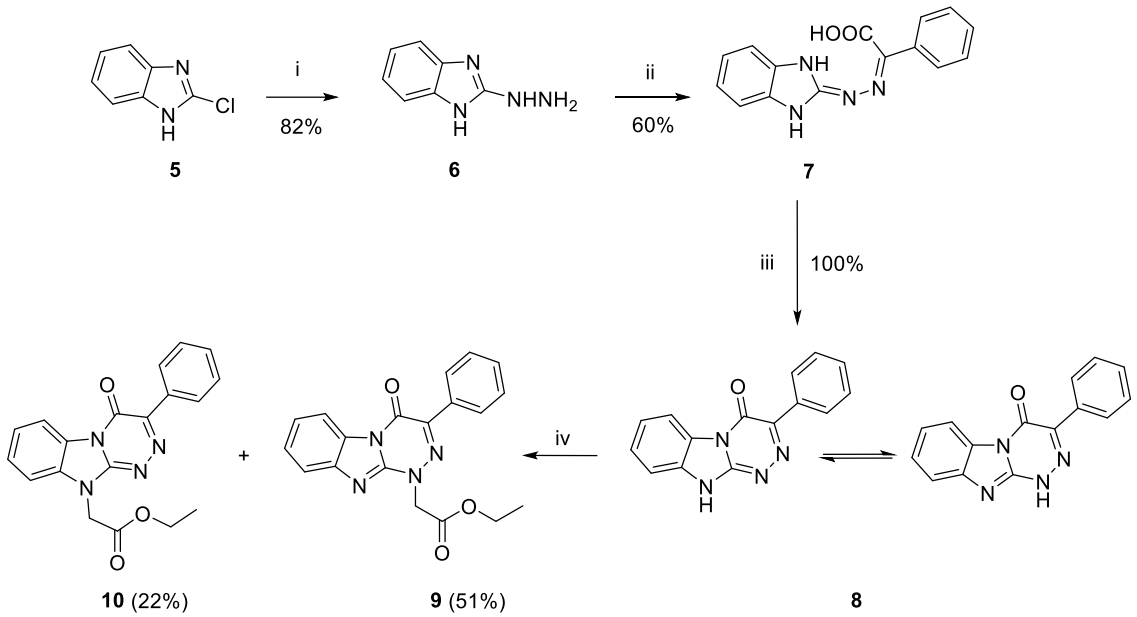

Reagents and conditions: **i**) hydrazine monohydrate, 180 °C, 5h; **ii**) phenylglyoxylic acid, absolute ethanol, 80 °C, 2h; **iii**) glacial acetic acid, 120 °C, 12h; **iv**) NaH, ethyl bromoacetate, anhydrous DMF, room temperature, overnight.

Because of the high similarity of the ^{1}H-NMR and ^{13}C-NMR spectra (see Experimental Section) of regioisomers **9** and **10**, these structures were unequivocally attributed by the synthesis of compound **10** following the procedure reported in Scheme 2, and subsequent HPLC analysis. The commercial 2-chlorobenzimidazole (**5**) was firstly *N*-alkylated to compound **11** with ethyl bromoacetate and sodium hydride. Subsequent treatment with hydrazine monohydrate furnished derivative **12**, which was directly reacted with phenylglyoxylic acid in absolute ethanol. In these experimental conditions, we directly obtained the cyclized compound **10**. HPLC analysis, performed with the mobile phase delivered at isocratic flow and consisting of acetonitrile (70%) and water (30%) and a flow rate of 1.0 mL/min, revealed a retention time for compound **10** of 5.6 min, with a purity degree > 95%. HPLC analysis repeated in the same conditions for regioisomers **9** and **10**, both in mixture and after separation by flash chromatography, revealed different retention times for compounds **9** and **10** (8.3 min and 5.6 min, respectively), allowing their structural assignment (chromatograms are reported in Fig. S1, S2, S3, S4, Supplementary Data).

Scheme 2

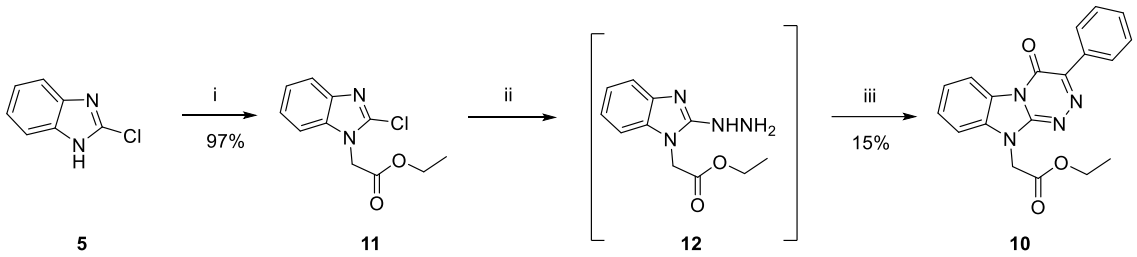

Reagents and conditions: **i**) NaH, ethyl bromoacetate, anhydrous DMF, room temperature, 3h; **ii**) hydrazine monohydrate, 180 °C, 5h; **iii**) phenylglyoxylic acid, absolute ethanol, 80 °C, 2h.

The synthetic procedure for the obtainment of N^1- and N^{10}-substituted derivatives (**1**,**2** and **3**,**4**, respectively) is outlined in Scheme 3.

Scheme 3

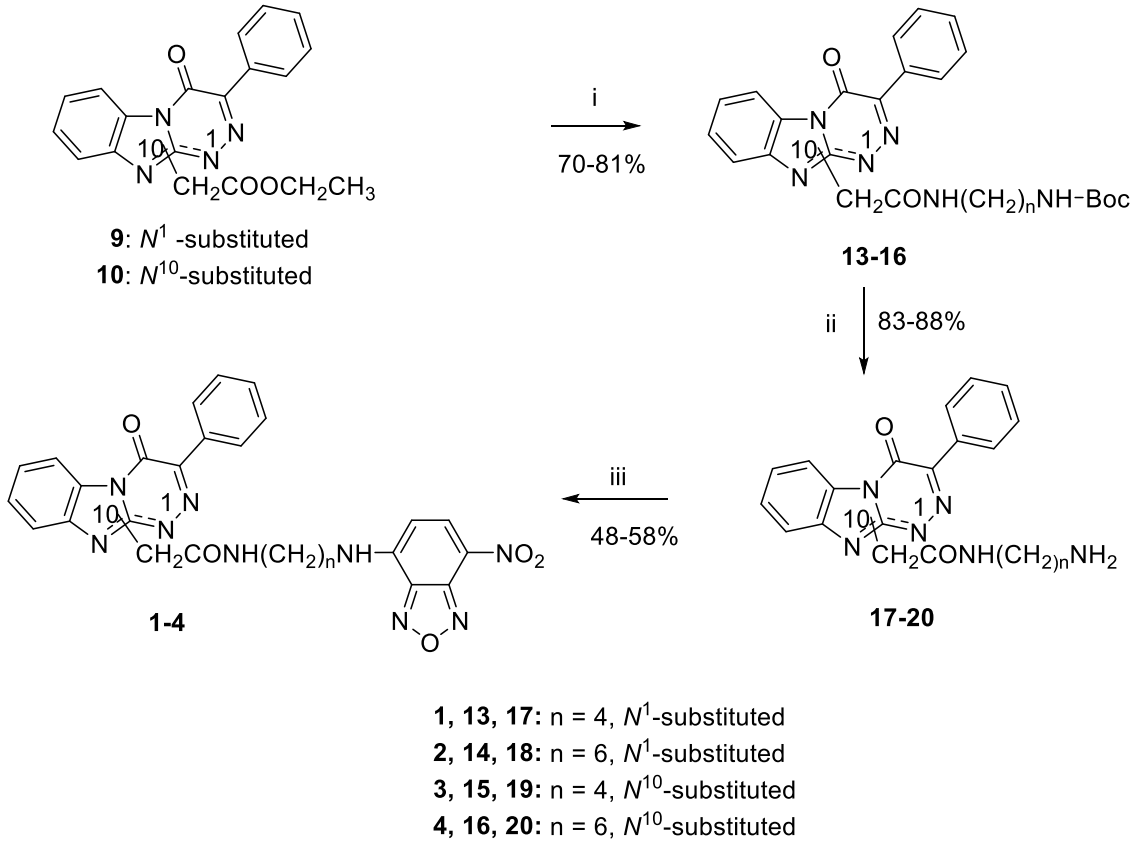

1, 13, 17: n = 4, N^1-substituted
2, 14, 18: n = 6, N^1-substituted
3, 15, 19: n = 4, N^{10}-substituted
4, 16, 20: n = 6, N^{10}-substituted

Reagents and conditions: **i**) *N*-Boc-1,4-butanediamine or *N*-Boc-1,6-hexanediamine, 80 °C, 3h; **ii**) trifluoroacetic acid, DCM, room temperature, 2h; **iii**) NBD-Cl, NEt_3, anhydrous DMF, room temperature, overnight.

Compound **9** and **10** were condensed with *N*-Boc-1,4-butanediamine and *N*-Boc-1,6-hexanediamine in a Pyrex capped tube at 80 °C for 3 hours to obtain derivatives **13-16**. Simple deprotection of the BOC group with trifluoroacetic acid in DCM gave the amino derivatives **17-20**, which were then reacted with the commercial 4-chloro-7-nitrobenzofurazan (NBD-Cl) in anhydrous DMF, in the presence of triethylamine, yielding the targets fluorescent probes **1-4**, finally purified by flash-chromatography.

*2.2. Binding profile of compounds **1-4** to adenosine receptors.*

The affinities of **1-4** for human A_1 and A_{2A} ARs were evaluated in competition binding experiments by assessing their abilities to displace [^{3}H]8-cyclopentyl-1,3-dipropylxanthine ([^{3}H]DPCPX) and [^{3}H]5′-N-ethylcarboxamideadenosine ([^{3}H]NECA) binding from transfected CHO cells, respectively. The experiments were performed as described elsewhere.[34] The ability of **1-4** to bind to A_3 AR was evaluated through functional assays.[21] The binding data of **1-4** at the human A_1, A_{2A}, and A_3 ARs are summarized in Table 1, together with those of the parent compound **8**,[18] DPCPX, NECA, and Cl-IBMECA reported as references.

Table 1. Binding of the triazinobenzimidazole derivatives **8**, **1-4** at human A_1, A_{2A} and A_3 ARs.[a]

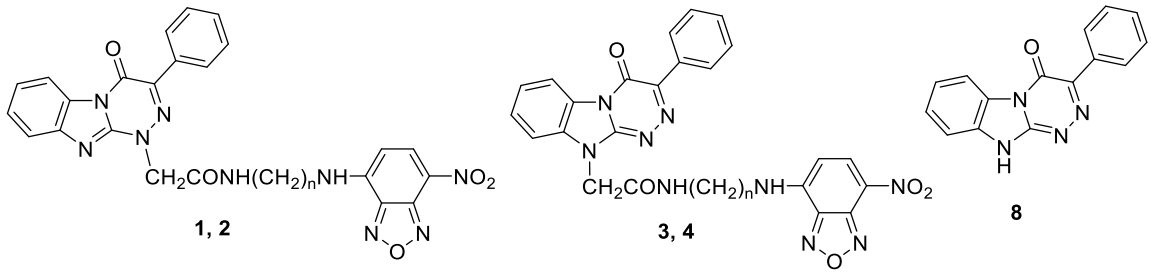

cpd	n	*h*A_1	*h*A_{2A}	*h*A_3	
		K_i (nM)[a,b]	K_i (nM)[a,c]	K_i (nM)[a,d]	IC_{50} (nM)[a,e]
8[f]	-	728 ± 38	> 10,000	> 1,000	-
1	4	> 10,000	> 10,000	-	> 10,000
2	6	> 10,000	> 10,000	-	> 10,000
3	4	1380 ±120	> 10,000	-	> 10,000
4	6	> 10,000	> 10,000	-	> 10,000
DPCPX		0.5 ± 0.03	337 ± 28	> 1,000	-
NECA		14 ± 4	16 ± 3	73 ± 5	-
Cl-IBMECA		890 ± 61	401 ± 25	0.22 ± 0.02	-

[a]The K_i and IC_{50} values are the means ± SEM of at least three determinations derived from an iterative curve-fitting procedure (Prism program, GraphPad, San Diego, CA). [b]Displacement of specific [^{3}H]DPCPX binding in membranes obtained from *h*A_1 AR stably expressed in CHO cells. [c]Displacement of specific [^{3}H]NECA binding in membranes obtained from *h*A_{2A} AR stably expressed in CHO cells. [d]Displacement of specific [^{125}I]AB-MECA binding in membranes obtained from *h*A_3 AR stably expressed in CHO cells. [e] The IC_{50} values correspond to the concentrations reducing by 50% the effect of the selective A_3 AR agonist Cl-IB-MECA. [f]Data taken from ref. 18.

None of the new compounds displayed any significant binding affinity for A_1, A_{2A} and A_3 ARs, with the exception of **3** that showed micromolar affinity for A_1 AR (K_i 1380 nM). Functional cAMP assays demonstrated that **3** behaves as antagonist at A_1 AR (Fig. 1A). This compound was able to counteract the NECA-mediated inhibition of cAMP accumulation in human A_1 AR-transfected CHO cells in a concentration-dependent manner, with an IC_{50} value comparable with the K_i value measured in the binding assay (IC_{50} 1112 nM).

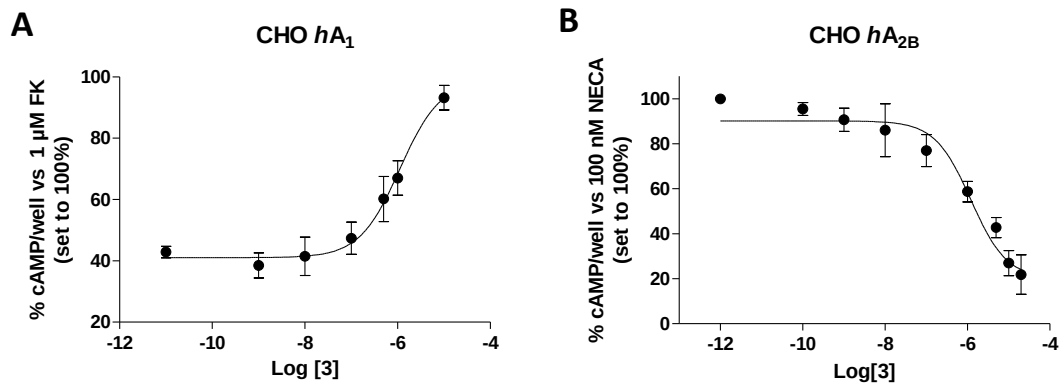

Figure 1. Evaluation of the antagonist profile of **3** towards the A_1 and A_{2B} AR subtypes. A) A_1 AR transfected CHO cells were treated with 1 µM forskolin and 10 nM NECA in the absence or presence of different concentrations of the tested compound (1 nM-10 µM). Data are expressed as the percentage of cAMP intracellular levels with respect to forskolin, which was set to 100%, and represent the mean ± SEM of at least three different experiments. Each experiment was performed in duplicate. B) A_{2B} AR-transfected CHO cells were treated with EC_{50} NECA concentration (100 nM) in the absence or presence of different concentrations (0.01 nM–10 µM) of the tested compound. After 15 min incubation, the reaction was stopped and the intracellular cAMP levels were quantified. The results are expressed as the percentage of NECA-stimulated cAMP levels, which was set to 100%. The data represent the mean ± SEM of at least three different experiments, each performed in duplicate.

Compounds **1**-**4** were then evaluated for their ability to modulate the increase in cAMP levels, either alone or in the presence of an EC_{50} concentration of the agonist NECA in human A_{2B} AR-transfected CHO cells (Table 2). When tested alone at a 10 µM concentration, all the compounds did not significantly increase cAMP levels, demonstrating a lack of A_{2B} AR agonist activity. Compounds **1** and **3** significantly counteracted the NECA-mediated increase in cAMP, suggesting that they may act as A_{2B} AR antagonists (Table 2).

Table 2. Effects of triazinobenzimidazole derivatives **1**-**4** on cAMP production in CHO cells expressing human A_{2B} AR.[a]

cpd	% cAMP production (vs agonist maximal effect, 100%)[b]	
	***h*A$_{2B}$ AR**	
	– agonist	+ agonist
1	3.4 ± 1.2	66.3 ± 4.5*
2	5.1 ± 2.1	101.0 ± 7.4
3	1.2 ± 0.8	20.7 ± 7.5***
4	1.7 ± 1.4	89.6 ± 6.5

[a] Each compound was tested at 10 μM concentration on cAMP production in CHO cells expressing human A_{2B} ARs (see Biology section). Each compound was tested alone or in the presence of 100 nM of NECA. [b] Data are expressed as percentage of cAMP production versus agonist maximal effect (100%). All data represent the mean ± SEM of at least three different experiments each performed in duplicate. *P<0.05, ***P<0.001 vs agonist alone.

Next, the potency of **1** and **3** for AR_{2B} AR was assessed. Compound **1** did not entirely counteract the NECA-induced cAMP production; thus, its IC_{50} value in this experiment could not be determined (>10,000 nM). Conversely, compound **3** completely counteracted the NECA-mediated increase of cAMP accumulation in human A_{2B} AR-transfected CHO cells, in a concentration-dependent manner (Fig. 1B), with an IC_{50} value in the micromolar range (IC_{50} 1350 nM). The presence of the NBD fluorophore significantly affected **3** potency towards A_{2B} AR with respect to its parent compound **8** (IC_{50} 1.40 nM).[18] These results suggested that the side chain bearing the NBD moiety is hosted in a lipophilic pocket of limited dimensions, such as to allow a moderate interaction only to the shortest linker at 10-position.

Given the ability of **3** to bind to A_1 and A_{2B} ARs in functional assays, this compound was investigated for its spectroscopic properties to evaluate its potential to visualize ligand-receptor interactions.

*2.3. Spectroscopic properties of the fluorescent probe **3**.*

The UV and the emission spectra of **3** were measured to investigate the spectroscopic properties of this compound as a fluorescent probe and how these might be affected by the chemical environment. Compound **3**, dissolved in dimethyl sulfoxide (DMSO), was

diluted to a final concentration of 10 µM in different assay solutions (from aqueous to 60% v/v dioxane-water phosphate-buffered saline (PBS)). The percentage of DMSO did not exceed 1% of the final assay volume solution.

Fig. 2A shows the absorption spectra of **3**. In an aqueous solution, the absorption spectrum of this compound is characterized by two absorption maxima at 366 and 478 nm with extinction coefficients of ε = 10286 M^{-1} cm^{-1} and ε = 8857 M^{-1} cm^{-1}, respectively. When **3** was dissolved in the PBS solution containing 20% of dioxane, the wavelengths of the absorption maxima remained nearly unchanged, but the spectrum was characterized by an increase in both extinction coefficients; this effect was much more evident at the longer wavelength. A further increase in hydrophobicity of the medium (40% dioxane/water (v/v) PBS or 60% dioxane/water (v/v) PBS) caused a slight increase in the extinction coefficients.

Fig. 2B shows the emission spectra of **3**. As expected, the decrease in polarity of the environment (from aqueous buffer to 60% dioxane in PBS) induced a 10-fold increase in quantum yield (Table 3). The maximum wavelength of emission is in the range of 538-542 nm for all the assay solutions. The same trend was also observed when the emission of compound **3** was recorded at 5 µM concentration (Figure S5, Supplementary Data).

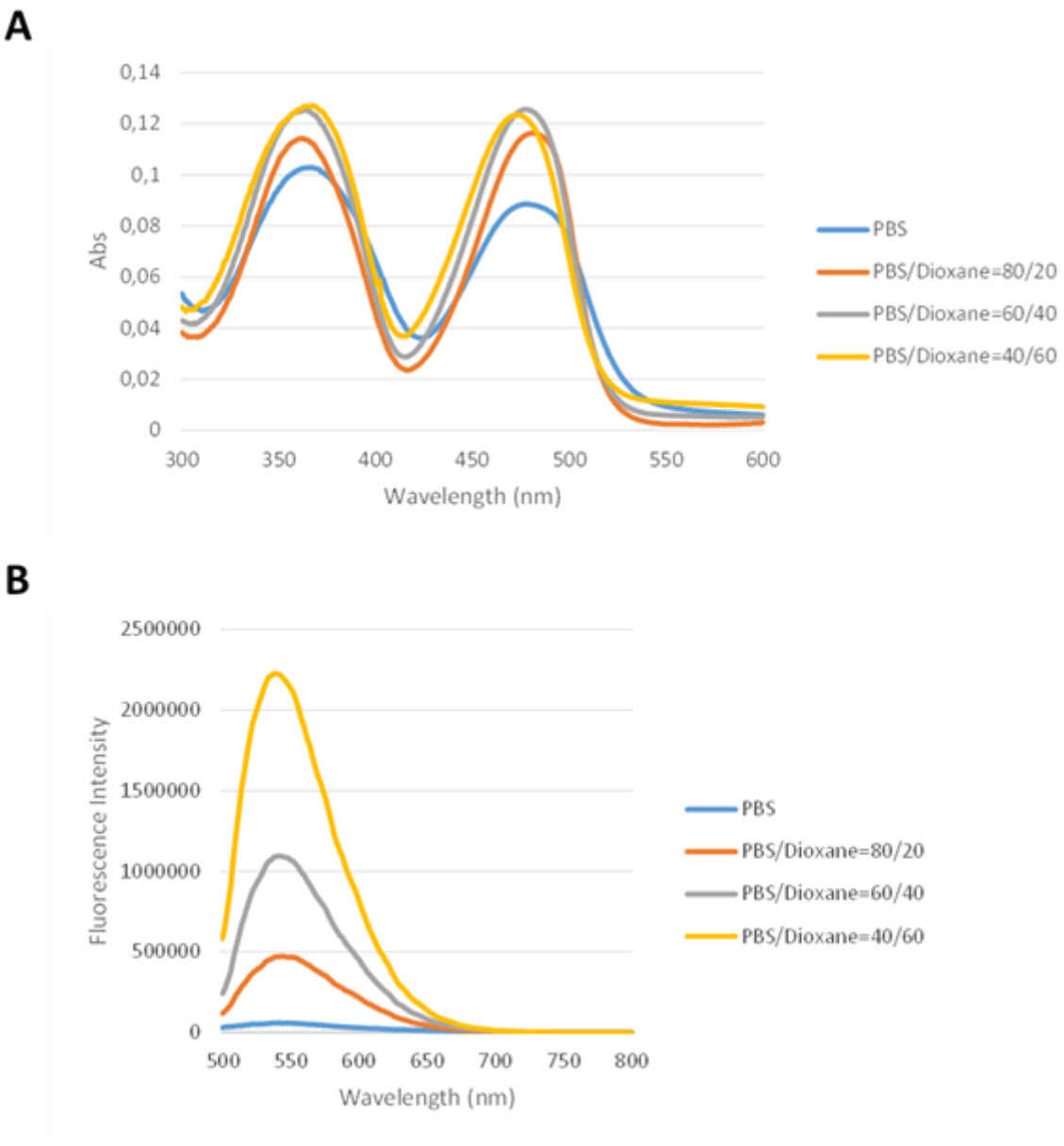

Figure 2. Absorption spectra of **3**. A) Acquisition of absorption spectra of **3** (10 μM) in solutions varying from aqueous to 60% dioxane-PBS (v/v) B) The influence of the

polarity of the medium on the fluorescence of **3** was investigated by addition of dioxane (indicated in % v/v) in PBS measured at a λ max of 366 nm.

Table 3. Quantum yield (Φ) of compound **3** in solutions varying from aqueous to 60% dioxane-PBS.

Solution	**Φ[a]**
PBS	0.0090
PBS/Dioxane 80/20	0.0124
PBS/Dioxane 60/40	0.0710
PBS/Dioxane 40/60	0.1352

[a]compared to the quinine bisulfate (in 0.1 N H_2SO_4, Φ=0.55)

*2.4. Fluorescent labelling of human BM-MSCs using compound **3**.*

Compound **3** was employed to visualize ligand-receptor interactions in undifferentiated BM-MSCs (Fig. 3). As previously reported, these cells express both A_{2B} and A_1 ARs,[25] so representing an effective cellular model to investigate the potential of **3** as a probe to visualize both the above mentioned AR subtypes.

The incubation of BM-MSCs with **3** resulted in a clear labelling of the cell (Fig. 3A,B), which was concentration-dependent. When the NBD was used alone, it was not able to bind BM-MSCs (Fig. S6). The co-labelling experiment with a specific membrane fluorescent dye (DiD) evidenced the AR localization on the BM-MSCs membrane (Fig. 3C). A substantial proportion of this binding was prevented by pre-incubation with the A_1 AR selective agonist R-PIA (100 nM, 10 min, 37 °C) and the A_{2B} AR agonist BAY 60-6583 (100 nM, 10 min, 37 °C) (Fig. 4B,C, Fig. S7). R-PIA alone significantly counteracted the specific binding of **3**, thus reducing the fluorescence of labelled BM-MSCs (Fig. 4A,B). Similarly, BAY 60-6583 alone significantly decreased the labelling

with **3** (Fig. 4A,B). The simultaneous occupation of the A_1 and A_{2B} AR binding sites caused a significant decrease of the fluorescent emission of **3** (Fig. 4A,B), demonstrating the specificity of the binding of **3** to A_1 and A_{2B} ARs.

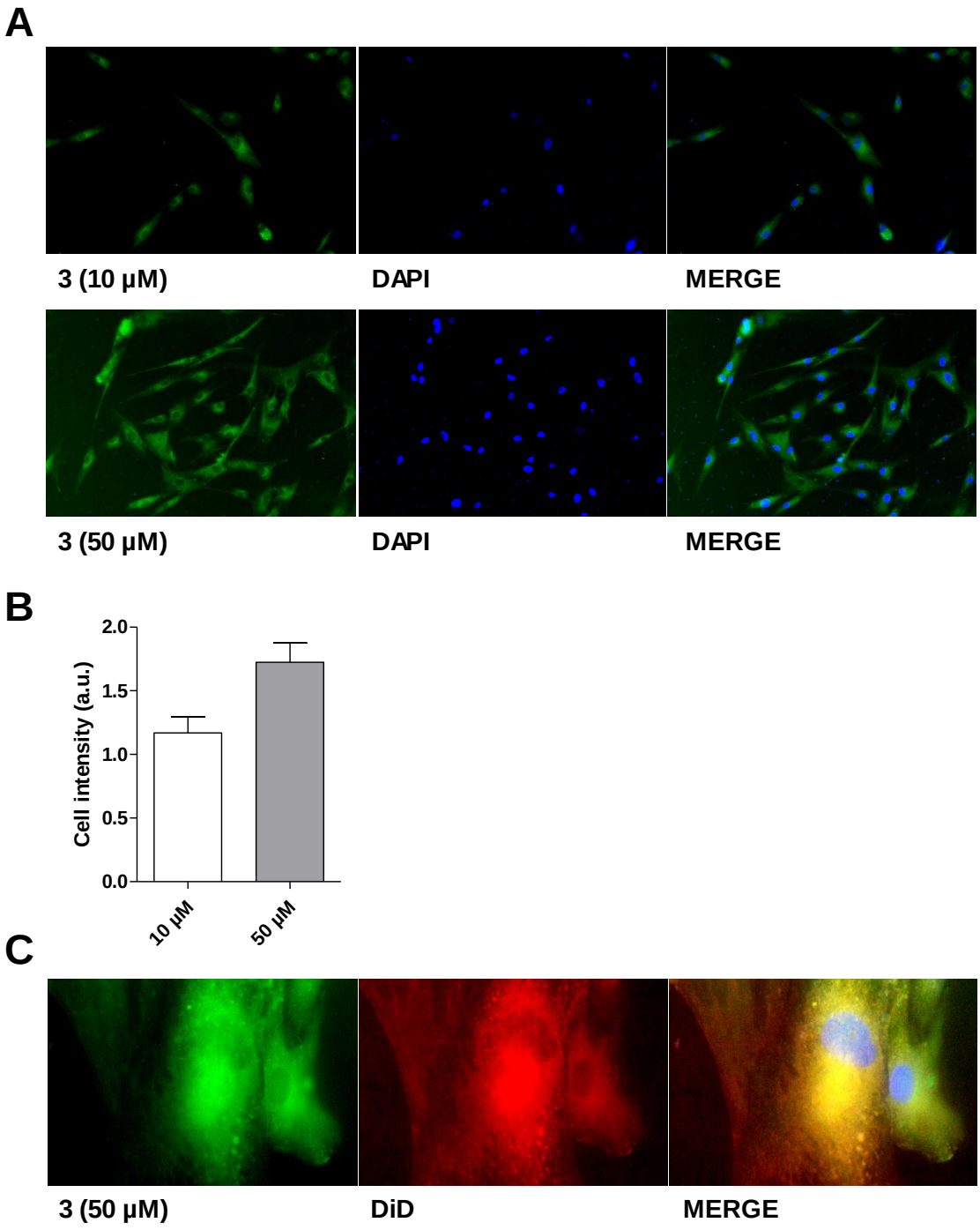

Figure 3. Fluorescence staining of BM-MSCs. A) Representative images of BM-MSCs treated with different concentrations of **3** (*in green*). Samples were fixed and imaged. Nuclei were counterstained with DAPI (*blue*). Scale bar = 250 μm. Two independent

experiments were performed in duplicate and five images were taken randomly for each sample. B) The mean intensity values of fluorescence were quantified. The data represent the mean ± SEM of five images with at least 25 cells. C) Representative images of BM-MSCs treated with **3** (in *green*) and DiD (in *red*). Samples were fixed and imaged. Nuclei were counterstained with DAPI (*blue*). Scale bar = 100 µm.

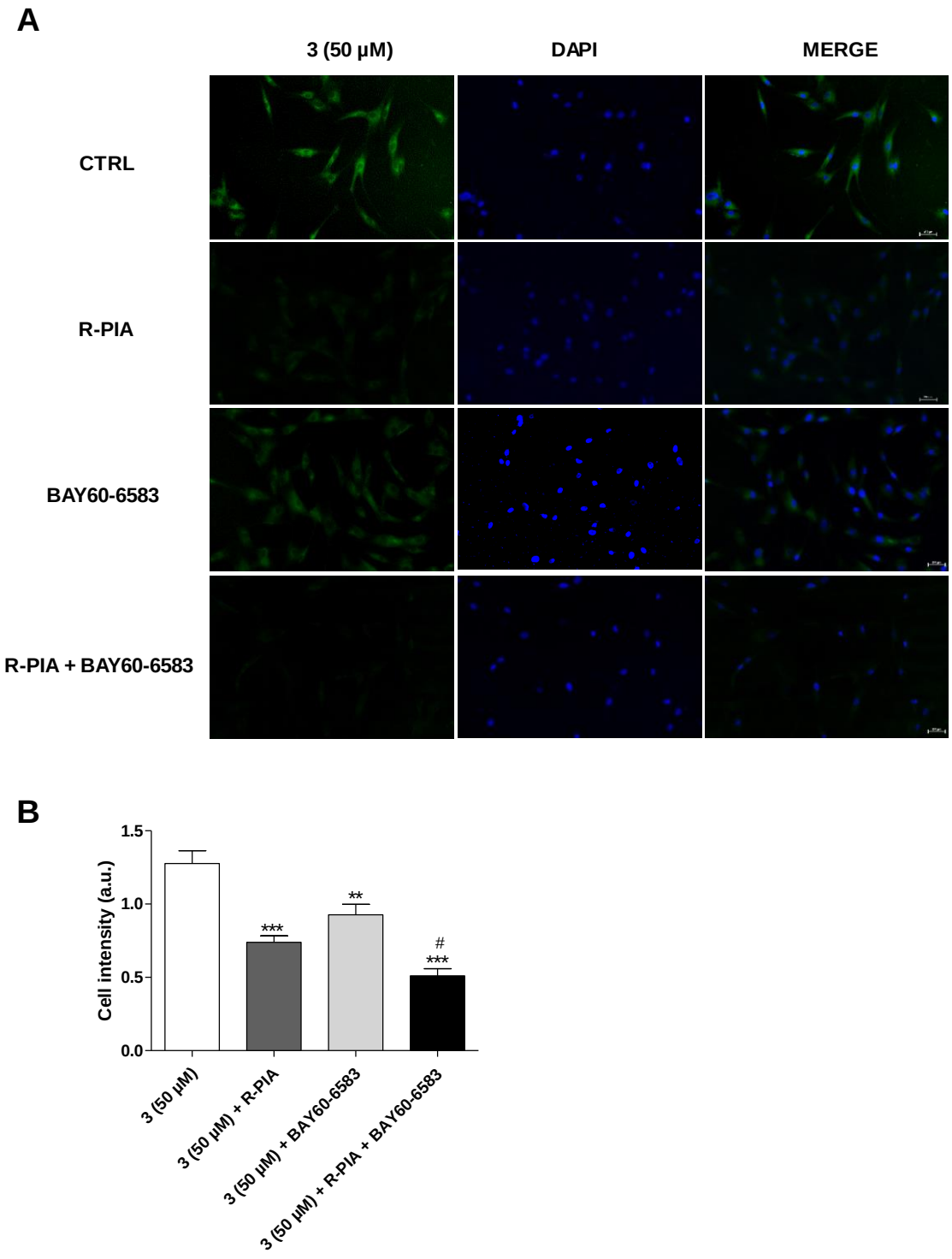

Figure 4. Fluorescent probe displacement in BM-MSCs. A) Representative images of BM-MSCs treated with: **3** (*green*, 50 µM), **3** + R-PIA (100 nM), **3** + BAY60-6583 (100

nM), **3** + R-PIA and BAY60-6583. Samples were fixed and imaged. Nuclei were counterstained with DAPI (*blue*). Scale bar = 250 μm. Two independent experiments were performed in duplicate and five images were taken randomly for each sample. B) The mean intensity values of fluorescence were quantified. The data represent the mean ± SEM of five images with at least 25 cells. The significance of the differences was determined by one-way ANOVA post hoc Bonferroni ** $P \leq 0.01$, *** $P \leq 0.001$ vs. **3**; # $P \leq 0.05$ vs. BAY alone.

3. Conclusions

In this study four green-emitting fluorescent triazinobenzimidazole derivatives were synthesized and characterized for their capability to interact with ARs. Among these, compound **3** demonstrated to act as A_1 and A_{2B} AR antagonist with similar binding affinity values for the two receptors. The results obtained from the staining of BM-MSCs with the fluorescent antagonist **3** resulted in clear labelling of the cell membrane, with a large proportion of this binding prevented by pre-incubation with the non-fluorescent R-PIA and BAY60-6583 as selective A_1 and A_{2B} AR agonists, respectively. Although further studies are needed to increase the selectivity of our triazinobenzimidazole derivatives for each AR subtype, these compounds could be useful to monitor the expression and localization of each AR subtype in several tissues and living cells in different physiological and pathological processes, such as MSC differentiation to osteoblasts and adipocytes.

4. Experimental Section

4.1. Chemistry.

4.1.1. General

The uncorrected melting points were determined using a Reichert Köfler hot-stage apparatus. NMR spectra were obtained on a Bruker AVANCE 400 or on Varian Gemini 200 spectrometer. The coupling constants are given in Hertz. Magnesium sulfate was used as the drying agent. Evaporations were made in vacuo (rotating evaporator).

Analytical TLC have been carried out on Merck 0.2 mm precoated silica gel aluminum sheets (60 F-254). Silica gel 60 (230–400 mesh) was used for column chromatography. Purity of the target inhibitors **1-4** was determined, using a Shimadzu LC-20AD SP liquid chromatograph equipped with a DDA Detector (λ = 254 nm) using a column C18 (250 mm x 4.6 mm, 5 μm, Shim-pack)). The mobile phase, delivered at isocratic flow, consisted of acetonitrile (60%) and water (40%) and a flow rate of 1.0 mL/min. All the

compounds showed percent purity values ≥ 95%. Fluorescence spectra were obtained by EnSight PerkinElmer. Absorption spectra were acquired by Victor Wallac 2 (Perkin Elmer).

Reagents, starting materials, and solvents were purchased from commercial suppliers and used as received. The following intermediates were obtained according to methods previously described: 2-hydrazinyl-1*H*-benzo[*d*]imidazole **6**, (Z)-2-(2-(1H-benzo[*d*]imidazol-2-yl)hydrazono)-2-phenylacetic acid **7** and 3-phenyl[1,2,4]triazino[4,3-a]benzimidazol-4(10*H*)-one **8**.[22]

*4.1.2. N-(4-((7-Nitrobenzo[c][1,2,5]oxadiazol-4-yl)amino)butyl)-2-(4-oxo-3-phenylbenzo[4,5]imidazo[2,1-c][1,2,4]triazin-1(4H)-yl)acetamide **1***. 4-Chloro-7-nitrobenzofurazan (0.056 g, 0.28 mmol) dissolved in 1 mL of anhydrous DMF was added dropwise to a stirred solution of derivative **17** (0.109 g, 0.28 mmol) in 10 mL of the same solvent, cooled at 0 °C, followed by addition of a solution of triethylamine (0.04 mL, 0.30 mmol). The reaction mixture was stirred at room temperature overnight and then concentrated in vacuo. The residue was taken up with 0 °C water and extracted with CH_2Cl_2 (3 × 40 mL). The combined organic phases were washed with brine, dried ($MgSO_4$), filtered, and concentrated in vacuo. Purification by column chromatography on silica gel (ethyl acetate as eluent) provided the target compound **1** as a yellow-brownish solid. Yield: 54%; m.p. = 182-184 °C; ^{1}H-NMR (DMSO-d_6, ppm): 1.51-1.58 (m, 2H); 1.67-1.74 (m, 2H); 3.18-3.22 (m, 2H); 3.41-3.46 (m, 2H); 5.12 (s, 2H); 6.31 (d, 1H, *J* = 8.0 *Hz*); 7.32-7.37 (m, 1H); 7.44-7.53 (m, 4H); 7.66 (d, 1H, *J* = 8.0 *Hz*); 8.03-8.06 (m, 2H); 8.26 (bs, 1H, exch D_2O); 8.31-8.34 (m, 2H); 9.46 (bs, 1H, exch D_2O). ^{13}C-NMR (DMSO-d_6, ppm): 25.29; 26.89; 38.54; 43.40; 56.19; 99.47; 115.29; 118.38; 120.96; 122.63; 127.01; 128.68 (2C); 128.85 (2C); 128.91; 129.95; 132.69; 137.84; 138.07; 141.78; 146.64; 152.44; 166.24. Anal. Calcd. for $C_{27}H_{23}N_9O_5$ (%): C, 58.59; H, 4.19; N, 22.77. Found: C, 58.41; H, 4.30; N, 22.80.

4.1.3. N-(6-((7-Nitrobenzo[c][1,2,5]oxadiazol-4-yl)amino)hexyl)-2-(4-oxo-3-phenylbenzo[4,5]imidazo[2,1-c][1,2,4]triazin-1(4H)-yl)acetamide **2**.

Compound **2** was obtained from derivative **18** (0.117 g, 0.28 mmol), according to the procedure described from amine **17**. Yield: 49%; m.p. = 123-125 °C; ^{1}H-NMR (DMSO-d_6, ppm): 1.29-1.33 (m, 4H); 1.38-1.45 (m, 2H); 1.60-1.64 (m, 2H); 3.10-3.15 (m, 2H); 3.39-3.43 (m, 2H); 5.11 (s, 2H); 6.32 (d, 1H, *J* = 8.0 *Hz*); 7.36-7.40 (m, 1H); 7.48-7.54

(m, 4H); 7.72 (d, 1H, *J* = 7.6 *Hz*); 8.03-8.05 (m, 2H); 8.19 (bs, 1H, exch D_2O); 8.36 (d, 1H, *J* = 8.0 *Hz*); 8.45 (d, 1H, *J* = 8.0 *Hz*); 9.50 (bs, 1H, exch D_2O).^{13}C-NMR (DMSO-d_6, ppm): 26.28; 26.44; 27.94; 29.31; 39.06; 43.65; 56.00; 99.41; 115.30; 118.47; 120.88; 122.66; 127.09; 128.69 (2C); 128.86 (2C); 128.94; 129.95; 132.70; 137.89; 138.28; 141.82; 146.72; 152.49; 166.06. Anal. Calcd. for $C_{29}H_{27}N_9O_5$ (%): C, 59.89; H, 4.68; N, 21.68. Found: C, 59.76; H, 4.74; N, 21.71.

4.1.4. N-(4-((7-Nitrobenzo[c][1,2,5]oxadiazol-4-yl)amino)butyl)-2-(4-oxo-3-phenylbenzo[4,5]imidazo[2,1-c][1,2,4]triazin-10(4H)-yl)acetamide **3**.

Compound **3** was obtained from derivative **19** (0.109 g, 0.28 mmol), according to the procedure described from amine **17**. Yield: 58%; m.p. = 253-255 °C; ^{1}H-NMR (DMSO-d_6, ppm): 1.53-1.56 (m, 2H); 1.68-1.71 (m, 2H); 3.16-3.21 (m, 2H), 3.45-3.49 (m, 2H); 5.11 (s, 2H); 6.39 (d, 1H, *J* = 8.0 *Hz*); 7.44-7.50 (m, 3H); 7.62-7.66 (m, 1H); 7.74 (d, 1H, *J* = 8.4 *Hz*); 7.96 (s, 1H); 8.15-8.17 (m, 2H); 8.35 (bs, 1H, exch D_2O); 8.44 (d, 1H, *J* = 9.2 *Hz*); 8.52 (d, 1H, *J* = 8.0 *Hz*); 9.53 (bs, 1H, exch D_2O). ^{13}C-NMR (DMSO-d_6, ppm): 24.42; 26.91; 38.62; 45.17; 46.02; 99.55; 110.97; 116.79; 120.99; 123.47; 124.91; 128.19; 128.48 (2C); 128.53 (2C); 129.37; 132.16; 134.50; 138.42; 145.60; 147.17; 150.40; 165.96. Anal. Calcd. for $C_{27}H_{23}N_9O_5$ (%): C, 58.59; H, 4.19; N, 22.77. Found: C, 58.45; H, 4.21; N, 22.86.

4.1.5. N-(6-((7-Nitrobenzo[c][1,2,5]oxadiazol-4-yl)amino)hexyl)-2-(4-oxo-3-phenylbenzo[4,5]imidazo[2,1-c][1,2,4]triazin-10(4H)-yl)acetamide **4**.

Compound **4** was obtained from derivative **20** (0.117 g, 0.28 mmol), according to the procedure described from amine **17**. Yield: 48%; m.p. = 211-213 °C; ^{1}H-NMR (DMSO-d_6, ppm): 1.30-1.37 (m, 4H); 1.43-1.46 (m, 2H); 1.62-1.67 (m, 2H); 3.10-3.15 (m, 2H); 3.41-3.45 (m, 2H); 5.10 (s, 2H); 6.34 (d, 1H, *J* = 8.0 *Hz*); 7.43-7.50 (m, 4H); 7.63-7.67 (m, 1H); 7.74 (d, 1H, *J* = 8.0 *Hz*); 8.16-8.18 (m, 2H); 8.31 (bs, 1H, exch D_2O); 8.44 (d, 1H, *J* = 8.8 *Hz*); 8.51 (d, 1H, *J* = 8.0 *Hz*); 9.51 (bs, 1H, exch D_2O). ^{13}C-NMR (DMSO-d_6, ppm): 26.27; 26.44; 28.01; 29.28; 39.11; 43.70; 45.19; 99.44; 110.99; 116.77; 120.86; 123.47; 124.92; 128.18; 128.47 (2C); 128.51 (2C); 129.34; 132.17; 134.55; 138.30; 145.57; 147.18; 150.41; 165.80. Anal. Calcd. for $C_{29}H_{27}N_9O_5$ (%): C, 59.89; H, 4.68; N, 21.68. Found: C, 59.78; H, 4.75; N, 21.70.

*4.1.6. Ethyl 2-(4-oxo-3-phenylbenzo[4,5]imidazo[2,1-c][1,2,4]triazin-(4H)-yl)acetate derivatives **9** and **10** (from Scheme 1).*

Sodium hydride suspension (60% suspension in paraffin oil) (0.120 g, 3.00 mmol) was added in small portions to a solution of 3-phenyl[1,2,4]triazino[4,3-*a*]benzimidazol-4(10*H*)-one **8** (0.787 g, 3.00 mmol) in 10 mL of anhydrous DMF, cooled at 0 °C. After the development of H_2 (about 1h), ethyl bromoacetate (0.33 mL, 3.00 mmol), dissolved in 2 mL of the same solvent, was added dropwise. The reaction mixture was maintained under stirring at room temperature for 24h (TLC analysis). The solution was dripped into ice and once the ice dissolved, the formed precipitate was collected by filtration and purified by flash chromatography (toluene:acetonitrile = 9:1 as eluent).

Ethyl 2-(4-oxo-3-phenylbenzo[4,5]imidazo[2,1-c][1,2,4]triazin-1(4H)-yl)acetate **9**. Yield: 51%; m.p. = 198-200 °C; ^{1}H-NMR (DMSO-d$_6$, ppm): 1.25 (t, 3H, *J* = 7.2 *Hz*); 4.23 (q, 2H, *J* = 7.2 *Hz*); 5.38 (s, 2H); 7.40-7.44 (m, 1H); 7.52-7.57 (m, 4H); 7.76 (d, 1H, *J* = 8.0 *Hz*); 8.04-8.06 (m, 2H); 8.38 (d, 1H, *J* = 8.0 *Hz*). ^{13}C-NMR (DMSO-d$_6$, ppm): 14.47; 54.60; 62.11; 115.44; 118.60; 122.91 (2C); 127.23; 128.72 (2C); 128.97 (2C); 130.11; 132.50; 138.11; 141.72; 146.39; 152.14; 167.74.

Ethyl 2-(4-oxo-3-phenylbenzo[4,5]imidazo[2,1-c][1,2,4]triazin-10(4H)-yl)acetate **10**. Yield: 22%; m.p. = 168-170 °C; ^{1}H-NMR (DMSO-d$_6$, ppm): 1.26 (t, 3H, *J* = 7.0 *Hz*); 4.23 (q, 2H, *J* = 7.2 *Hz*); 5.39 (s, 2H); 7.48-7.54 (m, 4H); 7.66-7.70 (m, 1H); 7.85 (d, 1H, *J* = 8.0 *Hz*); 8.17-8.20 (m, 2H); 8.52 (d, 1H, *J* = 8.0 *Hz*). ^{13}C-NMR (DMSO-d$_6$, ppm): 14.50; 43.90; 62.15; 111.06; 116.84; 123.73; 124.81; 128.31; 128.56 (2C); 128.64 (2C); 129.48; 131.68; 134.50; 146.20; 146.98; 150.36; 167.66.

4.1.7. Ethyl 2-(4-oxo-3-phenylbenzo[4,5]imidazo[2,1-c][1,2,4]triazin-10(4H)-yl)acetate **10** *(from Scheme 2).*

Compound **11** (0.400 g, 1.70 mmol) was heated at 180 °C in a Pyrex capped tube with 0.81 mL of hydrazine monohydrate (17.0 mmol) for 5 h. After the mixture was cooled, the precipitate, constituted by the 2-(2-hydrazinyl-1*H*-benzo[d]imidazol-1-yl)acetate **12**, was collected, dissolved in 10 mL of absolute ethanol and directly reacted added with phenyloxoacetic acid (0.255 g, 1.70 mmol), due to its scarce stability. The resulting mixture was refluxed for 5 h. After cooling, the solvent was removed under reduced pressure and the crude product was purified by column chromatography on silica gel (toluene:acetonitrile = 9:1 as eluent), furnishing **10** with low yield (15%).

4.1.8. Ethyl 2-(2-chloro-1H-benzo[d]imidazol-1-yl)acetate **11**.

Compound **11** was obtained from commercial 2-chlorobenzimidazole **5** (0.500 g, 3.30 mmol), sodium hydride suspension (60% suspension in paraffin oil) (0.132 g, 3.30 mmol) and ethyl bromoacetate (0.38 mL, 3.30 mmol), according to the procedure described for derivatives **9** and **10**. Yield: 97%; m.p. = 120-122 °C; ^{1}H-NMR (DMSO-d_6, ppm): 1.23 (t, 3H, *J* = 7.2 *Hz*); 4.20 (q, 2H, *J* = 7.2 *Hz*); 5.27 (s, 2H); 7.26-7.34 (m, 2H); 7.62-7.65 (m, 2H).

4.1.9. tert-Butyl(4-(2-(4-oxo-3-phenylbenzo[4,5]imidazo[2,1-c][1,2,4]triazin-1(4H)-yl)acetamido)butyl)carbamate **13.**

Compound **9** (0.209 g, 0.60 mmol) was heated at 80 °C in a Pyrex capped tube with *N*-Boc-1,4-butanediamine (0.226 g, 1.20 mmol) for 3h. The precipitate was dissolved with CH_2Cl_2 and washed with diluted (10%) HCl. After drying with $MgSO_4$, the dichloromethane solution was evaporated under reduced pressure, yielding the crude product that was purified by flash-chromatography (ethyl acetate:hexane = 5:5 as eluent). Yield: 79%; m.p. = 200-202 °C; ^{1}H-NMR (DMSO-d_6, ppm): 1.37-1.54 (m, 13H); 2.89-2.93 (m, 2H); 3.08-3.11 (m, 2H); 5.10 (s, 2H); 6.77 (bs, 1H, exch D_2O); 7.47-7.54 (m, 4H); 7.64-7.68 (m, 1H); 7.72-7.74 (m, 1H); 8.19-8.21 (m, 2H); 8.31 (bs, 1H, exch D_2O); 8.53 (d, 1H, *J* = 8.0 *Hz*).

4.1.10. tert-Butyl(6-(2-(4-oxo-3-phenylbenzo[4,5]imidazo[2,1-c][1,2,4]triazin-1(4H)-yl)acetamido)hexyl)carbamate **14**.

Compound **14** was obtained from ester **9** (0.209 g, 0.60 mmol) and *N*-Boc-1,6-hexanediamine (0.260 g, 1.20 mmol), according to the procedure described for amide **13**. Yield: 81%; m.p. = 205-207 °C; ^{1}H-NMR (DMSO-d_6, ppm): 1.22-1.24 (m, 4H); 1.36-1.44 (m, 13H); 2.85-2.92 (m, 2H); 3.09-3.10 (m, 2H); 5.10 (s, 2H); 6.75 (bs, 1H, exch D_2O); 7.40-7.45 (m, 1H); 7.51-7.58 (m, 4H); 7.74-7.76 (m, 1H); 8.03-8.06 (m, 2H); 8.16 (bs, 1H, exch D_2O); 8.40 (d, 1H, *J* = 7.6 *Hz*).

4.1.11. tert-Butyl(4-(2-(4-oxo-3-phenylbenzo[4,5]imidazo[2,1-c][1,2,4]triazin-10(4H)-yl)acetamido)butyl)carbamate **15**.

Compound **15** was obtained from ester **10** (0.209 g, 0.60 mmol) and *N*-Boc-1,4-butanediamine (0.226 g, 1.20 mmol), according to the procedure described for amide **13**. Yield: 70%; m.p. = 175-177 °C; ^{1}H-NMR (DMSO-d_6, ppm): 1.33-1.44 (m, 13H);

2.89-2.92 (m, 2H); 3.07-3.08 (m, 2H); 5.10 (s, 2H); 6.78 (bs, 1H, exch D_2O); 7.46-7.53 (m, 4H); 7.64-7.68 (m, 1H); 7.72-7.74 (m, 1H); 8.19-8.21 (m, 2H); 8.32 (bs, 1H, exch D_2O); 8.53 (d, 1H, *J* = 8.0 *Hz*).

4.1.12. tert-Butyl(6-(2-(4-oxo-3-phenylbenzo[4,5]imidazo[2,1-c][1,2,4]triazin-10(4H)-yl)acetamido)hexyl)carbamate **16**.

Compound **16** was obtained from ester **10** (0.209 g, 0.60 mmol) and *N*-Boc-1,6-hexanediamine (0.260 g, 1.20 mmol), according to the procedure described for amide **13**. Yield: 74%; m.p. = 185-187 °C; ^{1}H-NMR (DMSO-d_6, ppm): 1.21-1.26 (m, 4H); 1.32-1.43 (m, 13H); 2.85-2.90 (m, 2H); 3.07-3.10 (m, 2H); 5.10 (s, 2H); 6.76 (bs, 1H, exch D_2O); 7.47-7.54 (m, 4H); 7.64-7.68 (m, 1H); 7.72-7.72 (m, 1H); 8.19-8.21 (m, 2H); 8.30 (bs, 1H, exch D_2O); 8.52 (d, 1H, *J* = 8.0 *Hz*).

4.1.13. N-(4-Aminobutyl)-2-(4-oxo-3-phenylbenzo[4,5]imidazo[2,1-c][1,2,4]triazin-1(4H)-yl)acetamide **17.**

Trifluoroacetic acid (0.239 g, 2.10 mmol) was added to a stirred solution of derivative **13** (0.103 g, 0.21 mmol) dissolved in 10 mL of CH_2Cl_2. The reaction mixture was stirred at room temperature until the disappearance of the starting material (TLC analysis). After stirring at room temperature for 3 h, the reaction mixture was concentrated in vacuo. The solid residue was taken up with water, cooled in an ice bath, treated with a 3 M solution of NaOH, and extracted with CH_2Cl_2 (3 × 40 mL). The combined organic phases were washed with brine, dried ($MgSO_4$), filtered, and concentrated in vacuo to yield the title compound. Yield: 88%; m.p. = 144-146 °C; ^{1}H-NMR (DMSO-d_6, ppm): 1.46-1.50 (m, 4H); 2.71-2.74 (m, 2H); 3.12-3.13 (m, 2H); 5.11 (s, 2H); 7.42-7.45 (m, 1H); 7.52-7.59 (m, 4H); 7.75-7.77 (m, 1H); 8.04-8.06 (m, 2H); 8.26 (bs, 1H, exch D_2O); 8.41 (d, 1H, *J* = 8.0 *Hz*).

4.1.14. N-(6-Aminohexyl)-2-(4-oxo-3-phenylbenzo[4,5]imidazo[2,1-c][1,2,4]triazin-1(4H)-yl)acetamide **18**.

Compound **18** was obtained from derivative **14** (0.109 g, 0.21 mmol), according to the procedure described for amine **17**. Yield: 84%; m.p. = 178-180 °C; ^{1}H-NMR (DMSO-d_6, ppm): 1.36-1.40 (m, 8H); 2.67-2.69 (m, 2H); 3.07-3.09 (m, 2H); 5.09 (s, 2H); 7.40-7.42 (m, 1H); 7.51-7.56 (m, 4H); 7.72-7.73 (m, 1H); 7.99-8.01 (m, 2H); 8.14 (bs, 1H, exch D_2O); 8.37-8.40 (m, 1H).

4.1.15. N-(4-Aminobutyl)-2-(4-oxo-3-phenylbenzo[4,5]imidazo[2,1-c][1,2,4]triazin-10(4H)-yl)acetamide **19**.

Compound **19** was obtained from derivative **15** (0.103 g, 0.21 mmol), according to the procedure described for amine **17**. Yield: 87%; m.p. = 199-201 °C; ^{1}H-NMR (DMSO-d_6, ppm): 1.32-1.46 (m, 4H); 2.51-2.54 (m, 2H); 3.08-3.13 (m, 2H); 5.10 (s, 2H); 7.48-7.54 (m, 4H); 7.65-7.69 (m, 1H); 7.72-7.75 (m, 1H); 8.19-8.21 (m, 2H); 8.33 (bs, 1H, exch D_2O); 8.53 (d, 1H, *J* = 8.0 *Hz*).

4.1.16. N-(6-Aminohexyl)-2-(4-oxo-3-phenylbenzo[4,5]imidazo[2,1-c][1,2,4]triazin-10(4H)-yl)acetamide **20**.

Compound **20** was obtained from derivative **16** (0.109 g, 0.21 mmol), according to the procedure described for amine **17**. Yield: 83%; m.p. = 158-160 °C; ^{1}H-NMR (DMSO-d_6, ppm): 1.31-1.50 (m, 8H); 2.52-2.55 (m, 2H); 3.06-3.09 (m, 2H); 5.08 (s, 2H); 7.46-7.53 (m, 4H); 7.63-7.65 (m, 2H); 8.12-8.14 (m, 2H); 8.28 (bs, 1H, exch D_2O); 8.50 (d, 1H, *J* = 8.0 *Hz*).

4.2. **Determination of the Fluorescence Quantum Yield.**

The quantum yield of the probe (Φ_x) was determined according to equation:

$$\Phi_x = \Phi_{st}\left(\frac{D_x}{D_{st}}\right)\left(\frac{A_{st}}{A_x}\right)\left(\frac{\eta_x^2}{\eta_{st}^2}\right)$$

where the subscripts ST and X denote standard and test compound, respectively, Φ is the quantum yield, D is the area under the fluorescence emission spectra, A is the absorbance at the excitation wavelength, and η is the refractive index of the solvent used. Quinine bisulfate (Φf = 0.55 in 0.1 N H_2SO_4) is used as reference standard.

4.3. **Biology.**

4.3.1. Adenosine Receptor Binding Assay. Materials. [^{3}H]DPCPX and [^{3}H]NECA were obtained from DuPont-NEN (Boston, MA). ADA was from Sigma Chemical Co. (St. Louis, MO). All other reagents were from commercial sources and of the highest commercially available grade. CHO cells stably expressing human A_1, A_{2A}, A_3 and A_{2B} ARs were kindly supplied by Prof. K. N. Klotz, Wurzburg University, Germany.

4.3.2. Human A_1 Adenosine Receptors. Competition binding experiments were performed as previously reported (J. Med. Chem. 2012, 55, 1490−1499).[18] Briefly, membranes of A_1 CHO cells were incubated at 25 °C for 180 min in 500 μL of buffer containing [^{3}H]DPCPX (3 nM) and six different concentrations of the newly synthesized compounds. Nonspecific binding was determined in the presence of 50 μM RPIA. The dissociation constant (K_d) of [^{3}H]DPCPX in A_1 CHO cell membranes was 3 nM.

4.3.3. Human A_{2A} Adenosine Receptors. Competition binding experiments were performed as previously reported.[18] Briefly, membranes of A_{2A} CHO cells were incubated at 25 °C for 90 min in 500 μL of buffer in the presence of [^{3}H]NECA (30 nM) and six different concentrations of the newly synthesized compounds. Nonspecific binding was determined in the presence of 100 μM NECA. The dissociation constant (Kd) of [^{3}H]NECA in A_{2A} CHO cell membranes was 30 nM.

4.3.4. Measurement of Cyclic AMP Levels in A_1 AR, A_3 AR or A_{2B} AR CHO. Intracellular cyclic AMP (cAMP) levels were measured using a competitive protein binding method, as previously reported.[18] A_1 AR, A_3 AR or A_{2B} AR CHO cells were seed at a density of 48.000 cell/well in a 24 multiwell plate. After 48 h, the medium was removed, and the cells were incubated at 37 °C for 15 min with 0.5 mL of Dulbecco's Modified Eagle Medium (DMEM) in the presence of ADA (1U/mL) and the phosphodiesterase inhibitor Ro20-1724 (20 μM).

The agonist efficacy profile of the compounds at ARs was evaluated by assessing their ability to modulate intracellular cAMP levels in the absence of standard agonists; for the A_1 AR and A_3 AR, 1 μM forskolin a non-selective activator of adenylate cyclase were used. The antagonism profile of the new compounds was evaluated by assessing their ability to inhibit 100 nM NECA-mediated accumulation of cAMP for A_{2B} AR CHO cells; 10 nM NECA for A_1 AR CHO cells and 1 nM Cl-IBMECA for A_3 AR CHO cells. The new compounds were incubated 10 min before the addiction of the agonists. Then, cells were incubated in the reaction medium for 15 min at 37 °C. The reaction was stopped by the removal of the medium and the addition of 0.4 N HCl. After 30 min, lysates were neutralized with 4 N KOH, and the suspension was centrifuged at 800g for 5 min. For the determination of cAMP production, bovine adrenal cAMP binding protein was incubated with [^{3}H]cAMP (2 nM) and 50 μL of cell lysate or cAMP

standard (0−16 pmol) at 0 °C for 150 min in a total volume of 300 µL. Bound radioactivity was separated by rapid filtration through GF/C glass fiber filters and washed twice with 4 mL of 50 mM Tris/HCl, pH 7.4. The radioactivity was measured by liquid scintillation spectrometry.

4.3.5. Cell cultures

Human bone marrow derived MSCs were purchased by Lonza (Milan, Italy). Cells were cultured in normal growth medium (MSCGM, Lonza), plated (5.000 cells/cm^2) in 75-cm^2 flasks and incubated at 37 °C in 5% CO_2 and 95% air. The medium was changed to remove nonadherent cells every 3 to 4 days, and the cells were used at passages 2 to 5.

4.3.6. Immunofluorescent analysis.

MSCs were seeded at 10.000 cell/cm^2 in chamber slide (BD Biosciences, San Jose, CA, USA). Cells were treated with different concentrations of **3** for 10 min. In displacement experiments, R-PIA or BAY60-6583 for 10 min, then **3** was added for additional 10 min. Cell membranes were stained with DiD (10 µM, V-22887, ThermoFisher) for 20 min. After treatment, cells were fixed in 2% paraformaldehyde in 0.1 M phosphate buffer, washed three times with PBS, rinsed. After washing, nuclei were stained with DAPI (1:5000 dilution; Sigma–Aldrich) for 10 min. Then slides were covered with Vectashield (Vector Laboratories, Burlingame, CA, USA). Confocal images were acquired using a laser scanning confocal microscope TCS SP2 (Leica Microsystems, Germany) with a 40x oil immersion objective, at 1024x1024 pixel resolution. Each confocal image was a z-series, each averaged two times, and was chosen to cover the entire region of interest from top to bottom. The resulting z-stack was processed by Image J software (NIH) into a single image using "z-project" and "max intensity" options. Images were obtained with a Nikon Ni-E microscope, using a 20× objective with 1.45 NA and a recommended pinhole size of less than 1.0 micrometer, and equipped with digital camera Nikon Mod.DS-Ri2. Exposure time was set at 300 ms (DAPI) and 2 s (**3**) with the lamp intensity at 25%. The microscope, lamp, and camera settings were kept constant throughout this study. For presentation purposes, pictures were exported in TIFF format and processed with Adobe Photoshop, for adjustments of brightness and contrast. Quantification of the mean fluorescence intensity in selected regions was carried out by using the Fiji software as previously reported.[35] In brief, compound **3** signal was quantified as follows: the area covered by each cell was first

manually selected as a region of interest (ROI), then the ROI was applied to the correspondent compound **3** positive image and the intensity was measured by the ImageJ "Measure" tool (option "RawIntDen"). Then, the values were normalized to the mean Area and background fluorescence intensity were subtracted. Finally, the values were reported as Cell intensity (a.u.).

4.3.7. Statistical analysis.

The Graph-Pad Prism program (GraphPad Software Inc., San Diego, CA) was used for data analysis and graphic presentation. All data are the mean ± SEM. Statistical analysis was performed by one-way analysis of variance (ANOVA) with Bonferroni post-hot analysis. EC_{50} values were reported as mean of the values obtained in at least three independent experiments performed in duplicate ± SEM. $P \leq 0.05$ was considered statistically significant.

CONFLICT OF INTEREST

The authors declare no conflict of interest.

ACKNOWLEDGMENTS

We thank Prof. Claudia Gargini for her help in the acquisition and analysis of immunofluorescence images.

FUNDINGS

This work was supported by University of Pisa (PRA-project), and by the Italian Ministry of Education (Project of National Research Interest PRIN 2015, 2015E8EMCM_007).

References

1. Leopoldo M, Lacivita E, Berardi F, Perrone R. Developments in fluorescent probes for receptor research. *Drug Discov Today.* 2009;14(13-14): 706-712.
2. Briddon SJ, Kellam B, Hill SJ. Design and use of fluorescent ligands to study ligand-receptor interactions in single living cells. *Meth Mol Biol.* 2011;746: 211-236.
3. Duroux R, Ciancetta A, Mannes P, et al. Bitopic fluorescent antagonists of the A2A adenosine receptor based on pyrazolo[4,3-e][1,2,4]triazolo[1,5-c]pyrimidin-5-amine functionalized congeners. *MedChemComm.* 2017;8(8): 1659-1667.
4. Baker JG, Middleton R, Adams L, et al. Influence of fluorophore and linker composition on the pharmacology of fluorescent adenosine A1 receptor ligands. *Br J Pharmacol.* 2010;159(4): 772-786.
5. Köse M, Gollos S, Karcz T, et al. Fluorescent-labeled selective adenosine A2B receptor antagonist enables competition binding assay by flow cytometry. *J Med Chem.* 2018;61:4301-4316.
6. Fredholm BB, IJzerman AP, Jacobson KA, Klotz KN, Linden J. International Union of Pharmacology. XXV. Nomenclature and classification of adenosine receptors. *Pharmacol Rev.* 2001;53(4): 527-552.
7. Fredholm BB, IJzerman AP, Jacobson KA, Linden J, Muller CE. International Union of Basic and Clinical Pharmacology. LXXXI. Nomenclature and classification of adenosine receptors--an update. *Pharmacol Rev.* 2011;63(1): 1-34.
8. Zezula J, Freissmuth M. The A(2A)-adenosine receptor: a GPCR with unique features? *Br J Pharmacol.* 2008;153 Suppl 1: S184-190.
9. Langemeijer EV, Verzijl D, Dekker SJ, Ijzerman AP. Functional selectivity of adenosine A1 receptor ligands? *Purinergic Signal.* 2013;9(1): 91-100.
10. Giacomelli C, Daniele S, Romei C, et al. The A2B Adenosine Receptor Modulates the Epithelial- Mesenchymal Transition through the Balance of cAMP/PKA and MAPK/ERK Pathway Activation in Human Epithelial Lung Cells. *Front Pharmacol.* 2018;9: 54.
11. Da Settimo F, Primofiore G, Taliani S, et al. 3-Aryl[1,2,4]triazino[4,3-a]benzimidazol-4(10H)-ones: A New Class of Selective A1 Adenosine Receptor Antagonists. *J Med Chem.* 2001;44(3): 316-327.
12. Da Settimo F, Primofiore G, Taliani S, et al. A1 adenosine receptor antagonists, 3-aryl[1,2,4]triazino[4,3-a]benzimidazol-4-(10H)-ones (ATBIs) and N-alkyl and N-acyl-(7-substituted-2-phenylimidazo[1,2-a][1,3,5]triazin-4-yl)amines (ITAs): Different recognition of bovine and human binding sites. *Drug Dev Res.* 2004;63(1): 1-7.
13. Novellino E, Cosimelli B, Ehlardo M, et al. 2-(Benzimidazol-2-yl)quinoxalines: A Novel Class of Selective Antagonists at Human A1 and A3 Adenosine Receptors Designed by 3D Database Searching. *J Med Chem.* 2005;48(26): 8253-8260.
14. Da Settimo F, Primofiore G, Taliani S, et al. 5-Amino-2-phenyl[1,2,3]triazolo[1,2-a][1,2,4]benzotriazin-1-one: A Versatile Scaffold To Obtain Potent and Selective A3 Adenosine Receptor Antagonists. *J Med Chem.* 2007;50(23): 5676-5684.
15. Cosimelli B, Greco G, Ehlardo M, et al. Derivatives of 4-Amino-6-hydroxy-2-mercaptopyrimidine as Novel, Potent, and Selective A3 Adenosine Receptor Antagonists. *J Med Chem.* 2008;51(6): 1764-1770.
16. Taliani S, La Motta C, Mugnaini L, et al. Novel N2-substituted pyrazolo[3,4-d]pyrimidine adenosine A3 receptor antagonists: Inhibition of A3-mediated human glioblastoma cell proliferation. *J Med Chem.* 2010;53(10): 3954-3963.
17. Cosimelli B, Taliani S, Greco G, et al. Derivatives of Benzimidazol-2-ylquinoline and Benzimidazol-2-ylisoquinoline as Selective A1 Adenosine Receptor Antagonists with Stimulant Activity on Human Colon Motility. *ChemMedChem.* 2011;6(10): 1909-1918.

18. Taliani S, Pugliesi I, Barresi E, et al. 3-Aryl-[1,2,4]triazino[4,3-a]benzimidazol-4(10H)-one: A Novel Template for the Design of Highly Selective A2B Adenosine Receptor Antagonists. *J Med Chem.* 2012;55(4): 1490-1499.
19. Scatena A, Fornai F, Trincavelli ML, et al. 3-(Fur-2-yl)-10-(2-phenylethyl)-[1,2,4]triazino[4,3-a]benzimidazol-4(10H)-one, a Novel Adenosine Receptor Antagonist with A2A-Mediated Neuroprotective Effects. *ACS Chem Neurosci.* 2011;2(9): 526-535.
20. Rossi D, Nasti R, Marra A, et al. Enantiomeric 4-Acylamino-6-alkyloxy-2 Alkylthiopyrimidines As Potential A3 Adenosine Receptor Antagonists: HPLC Chiral Resolution and Absolute Configuration Assignment by a Full Set of Chiroptical Spectroscopy. *Chirality.* 2016;28(5): 434-440.
21. Cosimelli B, Greco G, Laneri S, et al. Studies on enantioselectivity of chiral 4-acetylamino-6-alkyloxy-2-alkylthiopyrimidines acting as antagonists of the human A3 adenosine receptor. *Med Chem Commun,.* 2018;9: 81-86.
22. Primofiore G, Da Settimo F, Taliani S, et al. 3-Aryl-[1,2,4]triazino[4,3-a]benzimidazol-4(10H)-ones: Tricyclic Heteroaromatic Derivatives as a New Class of Benzodiazepine Receptor Ligands. *J Med Chem.* 2000;43(1): 96-102.
23. Petroni D, Giacomelli C, Taliani S, et al. Toward PET imaging of A2B adenosine receptors: a carbon-11 labeled triazinobenzimidazole tracer. *Nucl Med Biol.* 2016;43(5): 309-317.
24. Gharibi B, Abraham AA, Ham J, Evans BA. Adenosine receptor subtype expression and activation influence the differentiation of mesenchymal stem cells to osteoblasts and adipocytes. *J Bone Miner Res.* 2011;26(9): 2112-2124.
25. Costa MA, Barbosa A, Neto E, et al. On the role of subtype selective adenosine receptor agonists during proliferation and osteogenic differentiation of human primary bone marrow stromal cells. *J Cell Physiol.* 2011;226(5): 1353-1366.
26. Trincavelli ML, Daniele S, Giacomelli C, et al. Osteoblast differentiation and survival: A role for A2B adenosine receptor allosteric modulators. *Biochim Biophys Acta, Mol Cell Res.* 2014;1843(12): 2957-2966.
27. D'Alimonte I, Nargi E, Lannutti A, et al. Adenosine A1 receptor stimulation enhances osteogenic differentiation of human dental pulp-derived mesenchymal stem cells via WNT signaling. *Stem Cell Res.* 2013;11(1): 611-624.
28. Eisenstein A, Ravid K. G protein-coupled receptors and adipogenesis: a focus on adenosine receptors. *J Cell Physiol.* 2014;229(4): 414-421.
29. Uchiyama S, Santa T, Okiyama N, Fukushima T, Imai K. Fluorogenic and fluorescent labeling reagents with a benzofurazan skeleton. *Biomed Chromatogr.* 2001;15(5): 295-318.
30. Taliani S, Simorini F, Sergianni V, et al. New fluorescent 2-phenylindolglyoxylamide derivatives as probes targeting the peripheral-type benzodiazepine receptor: design, synthesis, and biological evaluation. *J Med Chem.* 2007;50(2): 404-407.
31. Taliani S, Da Pozzo E, Bellandi M, et al. Novel irreversible fluorescent probes targeting the 18 kDa translocator protein: synthesis and biological characterization. *J Med Chem.* 2010;53(10): 4085-4093.
32. Milite C, Barresi E, Da Pozzo E, et al. Exploiting the 4-Phenylquinazoline Scaffold for the Development of High Affinity Fluorescent Probes for the Translocator Protein (TSPO). *J Med Chem.* 2017;60(18): 7897-7909.
33. Lin R, Angelin A, Da Settimo F, et.al. Genetic analysis of dTSPO, an outer mitochondrial membrane protein, reveals its functions in apoptosis, longevity, and Ab42-induced neurodegeneration. *Aging Cell.* 2014;13(3):507-518.
34. Cosimelli B, Greco G, Laneri S, et al. 4-amino-6-alkyloxy-2-alkylthiopyrimidine derivatives as novel non-nucleoside agonists for the adenosine A1 receptor. *Chem Biol Drug Des.* 2016;88(5): 724-729.
35. Schindelin J, Arganda-Carreras I, Frise E, et al. Fiji: an open-source platform for biological-image analysis. *Nat methods*. 2012;9(7):676-682.

Supplementary Data

SHIMADZU LabSolutions

Analysis Report

<Sample Information>

Sample Name	: Compound 9		
Sample ID	:		
Data Filename	:		
Method Filename	: AcCN70-H2O30.lcm		
Batch Filename	:		
Vial #	: 1-1	Sample Type	: Unknown
Injection Volume	: 1 uL		
Date Acquired	: 09/05/2018 15.15.09	Acquired by	: HPLC
Date Processed	: 16/05/2018 12.25.06	Processed by	: HPLC

<Chromatogram>

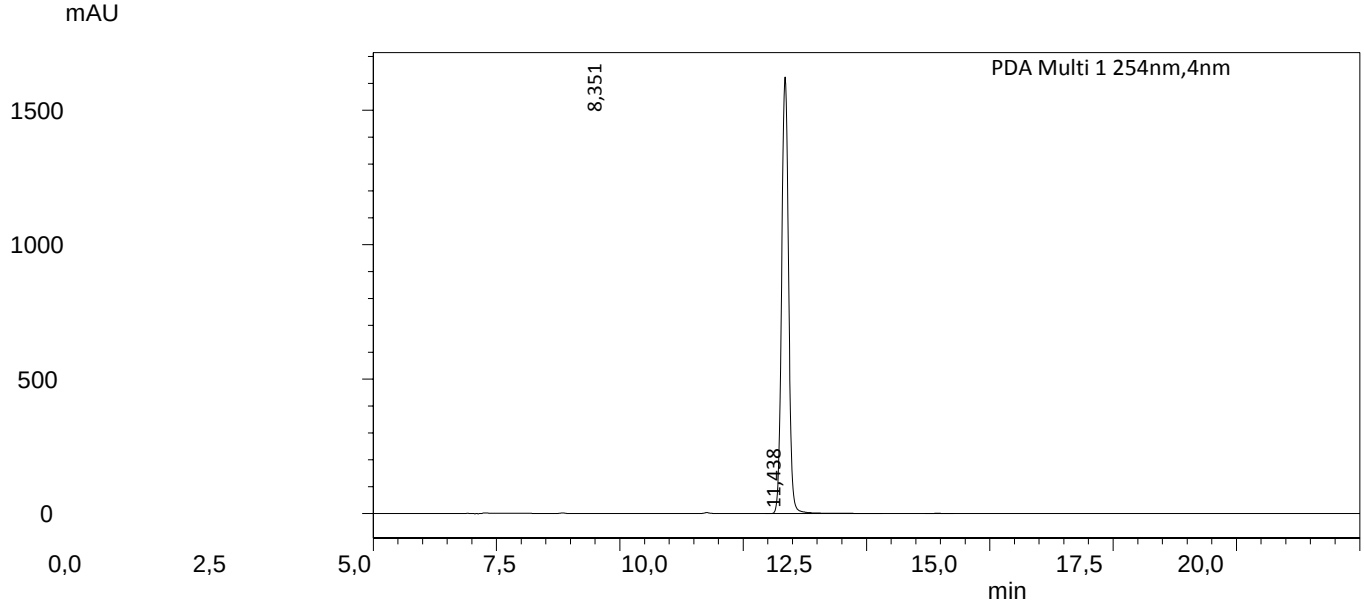

<Peak Table>

PDA Ch1 254nm

Peak#	Ret. Time	Area%
1	8,351	99,946
2	11,438	0,054
Total		100,000

Figure S1 Chromatogram of 9

SHIMADZU LabSolutions

Analysis Report

<Sample Information>

Sample Name	: Compound 10 from scheme 1		
Sample ID	:		
Data Filename	:		
Method Filename	: AcCN70-H2O30.lcm		
Batch Filename	:		
Vial #	: 1-1	Sample Type	: Unknown
Injection Volume	: 1 uL		
Date Acquired	: 14/05/2018 16.30.27	Acquired by	: HPLC
Date Processed	: 16/05/2018 12.26.02	Processed by	: HPLC

<Chromatogram>

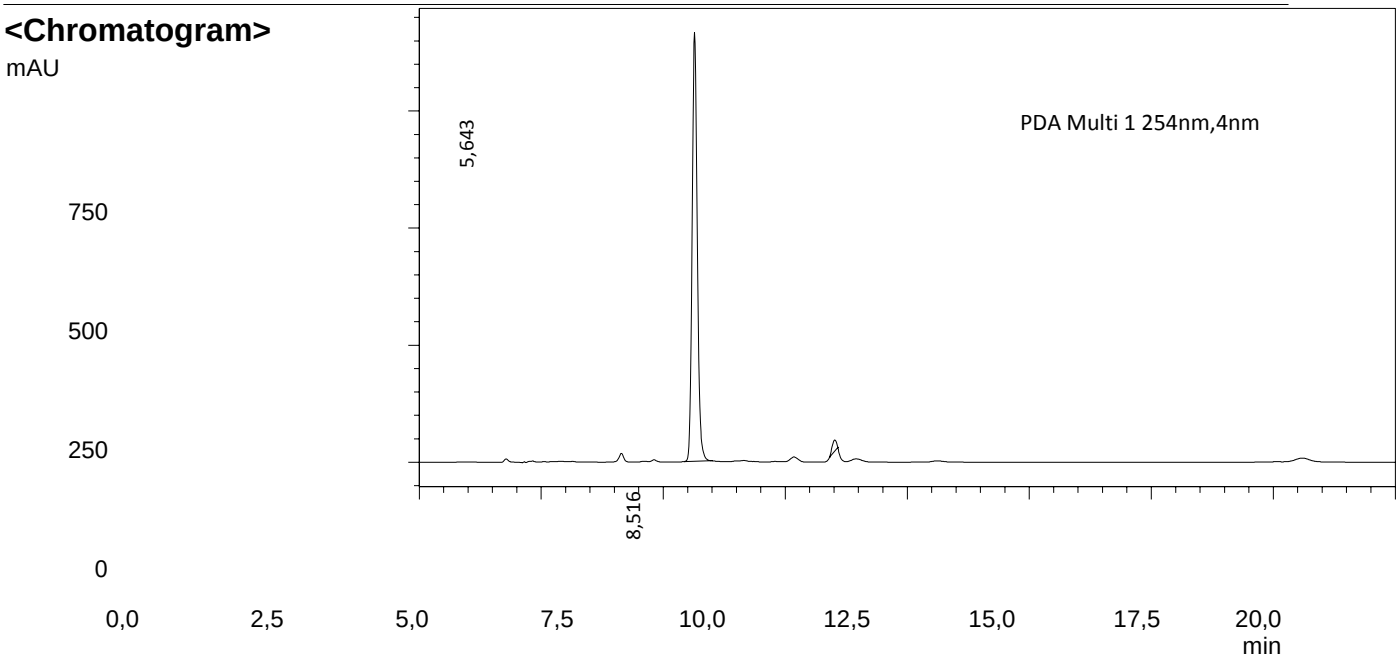

<Peak Table>

PDA Ch1 254nm

Peak#	Ret. Time	Area%
1	5,643	97,831
2	8,516	2,169
Total		100,000

Figure S2 Chromatogram of 10 from scheme 1

SHIMADZU LabSolutions

Analysis Report

<Sample Information>

Sample Name	: Compound 10 from scheme 2		
Sample ID	:		
Data Filename	:		
Method Filename	: AcCN70-H2O30.lcm		
Batch Filename	:		
Vial #	: 1-1	Sample Type	: Unknown
Injection Volume	: 1 uL		
Date Acquired	: 16/05/2018 11.27.49	Acquired by	: HPLC
Date Processed	: 16/05/2018 12.22.35	Processed by	: HPLC

<Chromatogram>

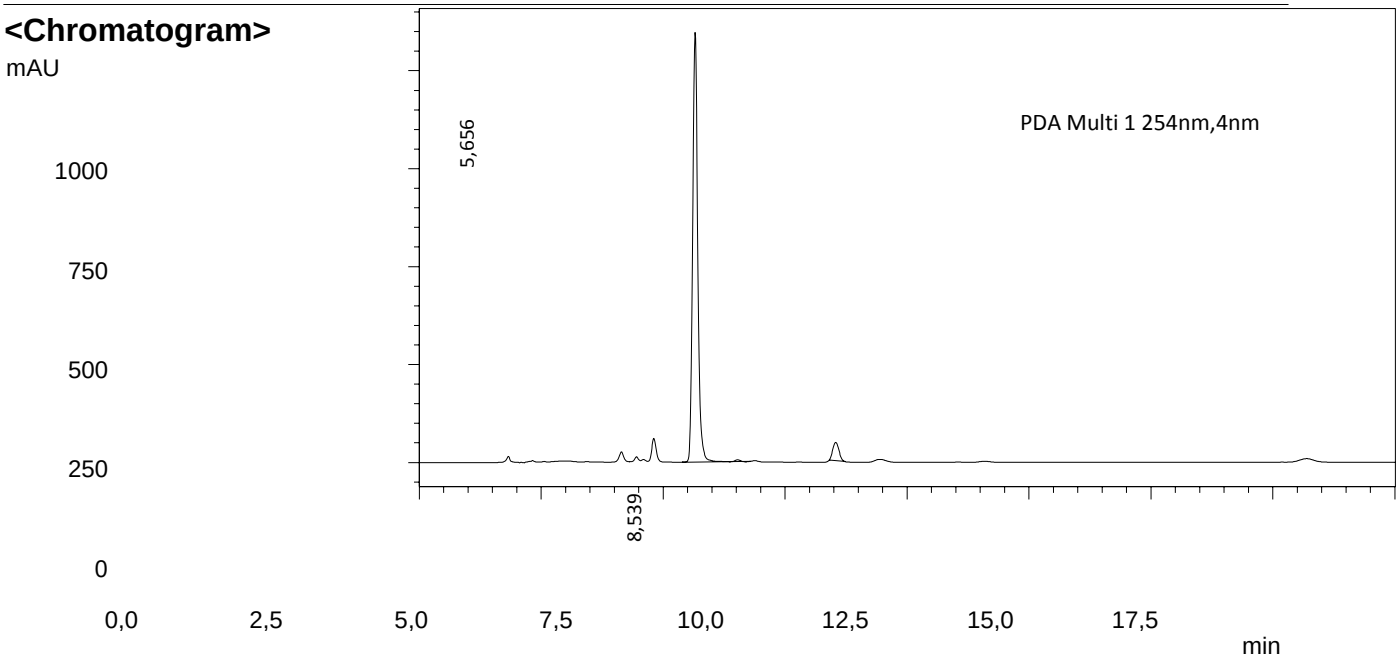

<Peak Table>

PDA Ch1 254nm

Peak#	Ret. Time	Area%
1	5,656	95,148
2	8,539	4,852
Total		100,000

Figure S3 Chromatogram of 10 from scheme 2

SHIMADZU LabSolutions

Analysis Report

<Sample Information>

Sample Name	: cpd 9 + cpd 10		
Sample ID	:		
Data Filename	:		
Method Filename	: AcCN70-H2O30.lcm		
Batch Filename	:		
Vial #	: 1-1	Sample Type	: Unknown
Injection Volume	: 1 uL		
Date Acquired	: 14/05/2018 15.57.19	Acquired by	: HPLC
Date Processed	: 16/05/2018 12.23.31	Processed by	: HPLC

<Chromatogram>

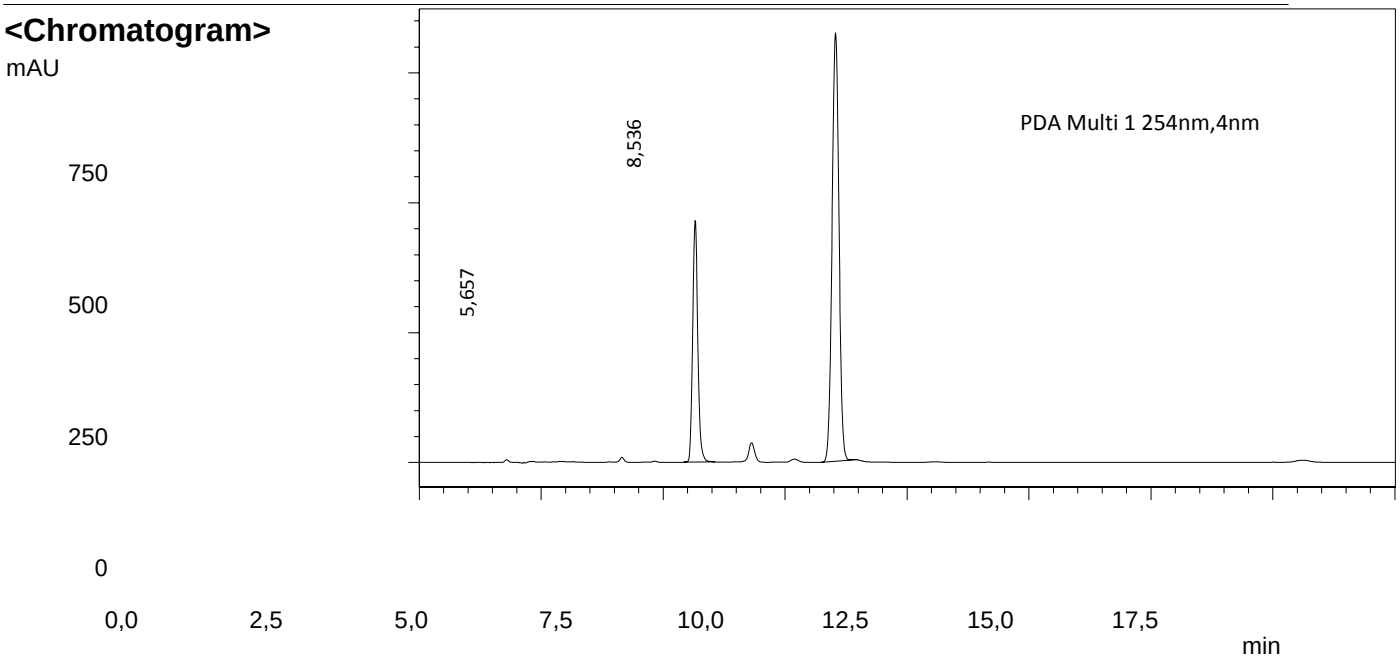

<Peak Table>

PDA Ch1 254nm

Peak#	Ret. Time	Area%
1	5,657	29,648
2	8,536	70,352
Total		100,000

Figure S4 Chromatogram of 9 + 10

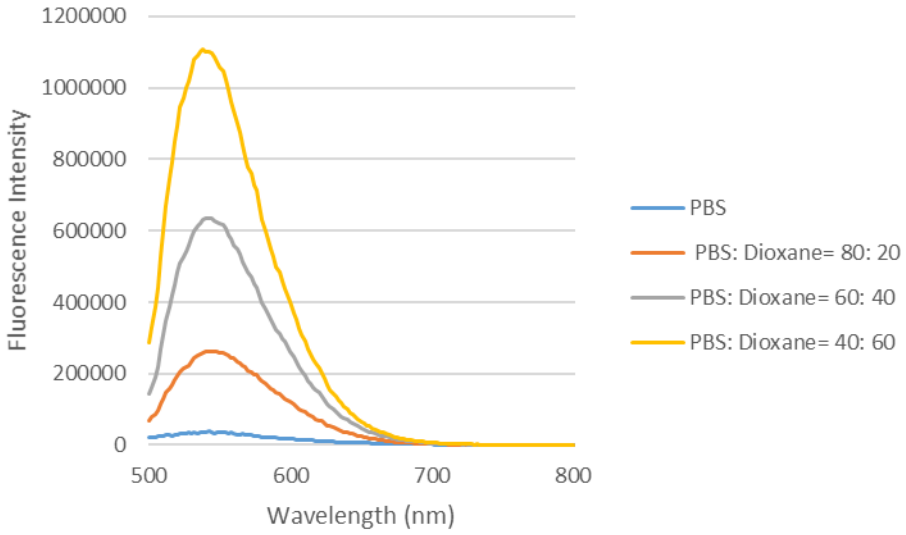

Figure S5 Emission spectra of 3 at 5 µM

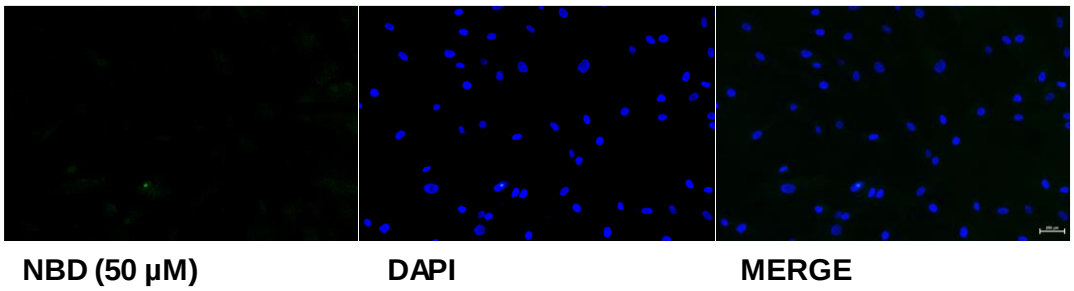

Figure S6 Fluorescence staining of BM-MSCs with NBD.

Representative images of BM-MSCs treated with NBD (in *green*). Samples were fixed and imaged at fluorescent microscope. Nuclei were counterstained with DAPI (*blue*). Bar = 250 µm.

A

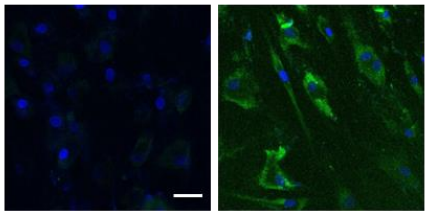
CTRL
3 (50 µM)

B

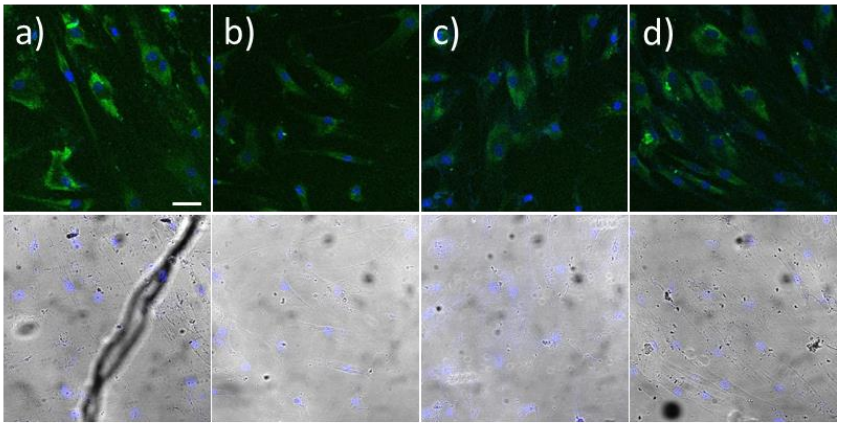
a)
b)
c)
d)

C

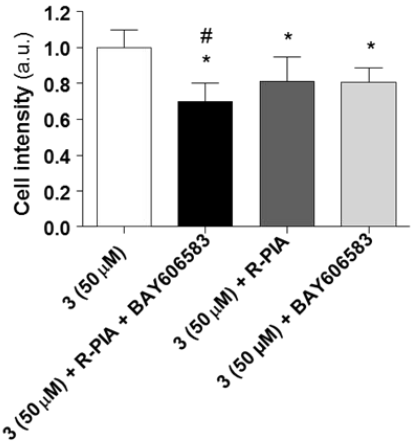
Cell Intensity (a.u.)
1.2
1.0
0.8
0.6
0.4
0.2
0.0
#
*
*
*
3 (50 µM)
3 (50 µM) + R-PIA + BAY606583
3 (50 µM) + R-PIA
3 (50 µM) + BAY606583

Figure S7 Fluorescence staining of BM-MSCs.

A) Representative images of BM-MSCs treated with 3 (in green). B) Representative images of BM-MSCs treated with: a) 3 (50 µM), b) 3 + R-PIA (100 nM) and BAY-606583 (100 nM), c) 3 + R-PIA, d) 3 + BAY-606583. Samples were fixed and imaged at confocal microscope. Nuclei were counterstained with DAPI (blue). Two independent experiments were performed in duplicate and five images were taken randomly for each sample. C) The mean intensity values of fluorescence were quantified. Data represent the mean ± SD. The significance of the differences was determined by Student-t-test, * $P \leq 0.05$ vs. 3; or with one-way ANOVA post hoc Dunnett's test # $P \leq 0.05$.